Research Article

Chemical Review and Letters
journal homepage: www.chemrevlett.com
ISSN (online): 2645-4947 (print) 2676-7279

Experimental and computational investigations of some new cabamothioate compounds

Nahid Shajari [a,*], Hooriye Yahyaei [a], and Ali Ramazani [b, c]

[a]*Department of Chemistry, Zanjan Branch, Islamic Azad University, P.O. Box 49195-467, Zanjan, Iran*
[b] *Department of Chemistry, University of Zanjan, P.O. Box 45195-313, Zanjan, Iran*
[c]*Research Institute of Modern Biological Techniques (RIMBT), University of Zanjan, P.O. Box 10 45195-313, Zanjan, Iran*

ARTICLE INFO

Article history:
Received 1 October 2020
Received in revised form 20 December 2020
Accepted 30 December 2020
Available online 1 January 2021

Keywords:
Trichloroacetyl isocyanate
Carbamothioate
Thiophenol
Naphthalenethiol
DOS
Vibrational frequencies
NMR chemical shift analysis

ABSTRACT

The new derivatives of *S*-aryl (trichloroacetyl) carbamothioate were prepared from a two-component reaction of 2-naphthalenethiol or thiophenol derivatives and trichloroacetyl isocyanate in CH_2Cl_2 at room temperature at high yields. The reaction was a simple and efficient procedure with high yield and available stating materials in a short time for the synthesis of these compounds that no side reactions were observed. The structures of the products were confirmed by IR, ^{1}H NMR, ^{13}C NMR spectroscopy, and elemental analysis. Quantum theoretical calculations for the three structures of compounds (3a, 3b and 3c) were performed using the G3MP2, LC-ωPBE, MP2, and B3LYP methods with the 6-311+G(d,p) basis set. Geometric parameters of optimized the structures were compared with the experimental measurements. The structures of the products were confirmed by IR, ^{1}H NMR, ^{13}C NMR, and elemental analysis. IR spectra data and ^{1}H NMR and ^{13}C NMR chemical shifts computations of the compounds were calculated. Frontier molecular orbitals (FMOs), total density of states (DOS), thermodynamic parameters and molecular electrostatic potentials (MEP) of the title compounds were investigated by theoretical calculations. Molecular properties such as the ionization potential (I), electron affinity (A), chemical hardness (η), electronic chemical potential (μ) and electrophilicity (ω) were investigated for the structures. Consequently, there was an excellent agreement between experimental and theoretical results.

1. Introduction

Carbamothioates are a family of organosulfur compounds that are also known as thiocarbamates. These are significant group of compounds that have many biological effects from pesticidal, fungicidal, bactericidal, anesthetic and antiviral activity, but the most famous applications of these compounds are their use as pesticides and especially as herbicides [1-5]. Furthermore *S*-alkyl (aryl) thiocarbamates are an important class of compounds for a variety of industrial, synthetic and medicinal applications. They have been broadly used as pharmaceuticals [6], Agrochemicals [7], and intermediates in organic synthesis [8] for the protection of amino groups in peptide chemistry [9]. *S*-Alkyl (aryl) thiocarbamates are usually produced from a two-step reaction using phosgene [10], its derivatives, and carbon monoxide [11]. Many reports show the intramolecular rearrangement of different derivatives to *S*-alkyl (aryl) thiocarbamates [12], in the presence of a catalyst elements such as palladium [13] nickel [14] and rhodium [15]. Because of our interest in the synthesis of sulfur and phosphorus compounds [16, 17]. We reported a two-component reaction, which, starting from readily available **t**richloroacetyl isocyanate and 2-naphthalenethiol or thiophenol derivatives affords 3a-c. (Scheme 1)

Computational chemistry is a subset of the science of chemistry and discusses the analysis and measurement of properties of materials that are not directly measurable and it utilizes other sciences such as mathematics and statistics. Computational organic chemistry is an important area in determining the mechanisms of che21mical reactions [18], especially catalysis [19], structural determination of organic compounds [20], prediction of spectroscopic data such as ^{1}H NMR and ^{13}C NMR chemical shifts [21], properties calculation of organic molecules [22-26], and the interaction of a

substrate with an enzyme [27]. This study has revealed some potential leads for possible pharmaceutical applications and further investigations may help in the development of new anti-oxidative agents for important metabolic functions. Furthermore, three new crystal structures of the compounds 3a, 3b and 3c have been reported. In the present work, we have investigated the energetic and structural properties of three compounds of 2-naphthalenethiol or thiophenol derivatives and trichloroacetyl isocyanate in CH_2Cl_2 occurs at room temperature, and the produced *S*-aryl (trichloroacetyl)carbamothioate derivatives (3a, 3b and 3c), which have been analyzed by means of the G3MP2, the long-range corrected version of the Perdew- Burke-Ernzerhof (PBE) exchange functional (LC-ωPBE), second-order Møller- Plesset perturbation theory (MP2) and hybrid density functional (B3LYP) based methods with the 6-311+G(d,p) basis set on all atoms. The optimized geometries, quantum molecular descriptors, IR spectra data, ^{1}H NMR and ^{13}C NMR chemical shifts computations, molecular electrostatic potentials (MEP), the thermodynamic and electronic properties and NBO analysis have been calculated and carried out.

2. Results and Discussion

The two-component reaction of 2-naphthalenethiol or thiophenol derivatives **(1)** and trichloroacetyl isocyanate **(2)** occurred in a 1:1 ratio in CH_2Cl_2 at room temperature, and the *S*-aryl (trichloroacetyl)carbamothioate derivatives **(3a-c)** were afforded in high yields, and fairly mild reaction conditions (Scheme 1 and Table 1). A mechanistic rationalization for this reaction is provided in Scheme 2.

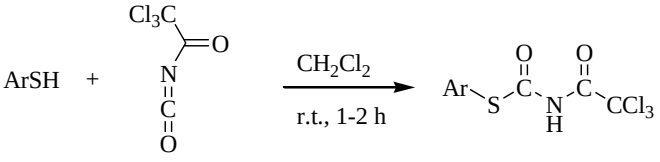

(1) **(2)** **(3a-c)**

Scheme 1. Two-component reaction of trichloroacetyl isocyanate with 2-naphthalenethiol or thiophenolderivatives **(3a-c)**.

Table 1. Synthesis of *S*-aryl (trichloroacetyl)carbamothioate derivatives **(3a-c)**.

Entry	Compounds	ArSH	Yield %
1	3a	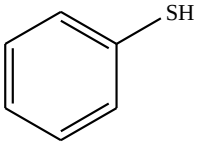	100
2	3b	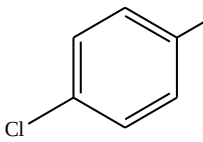	98
3	3c	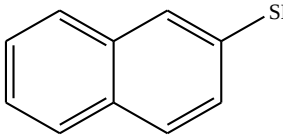	97

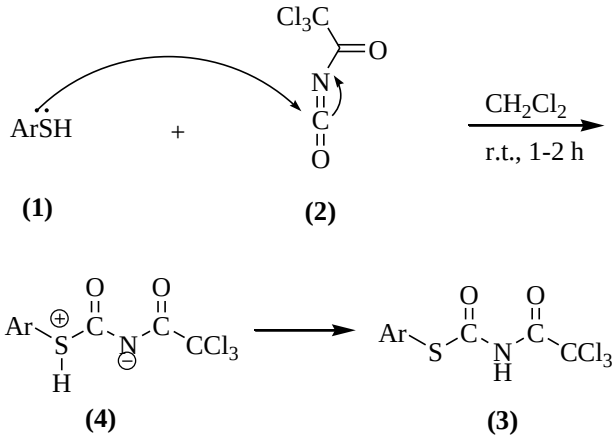

Scheme 2. A proposed mechanism for the formation of **(3).**

The structures of the products were deduced from their ^{1}H-NMR, ^{13}C-NMR, IR spectra, and elemental analysis. For example the ^{1}H-NMR spectrum of **3a** exhibited distinct signals at δ_H 7.40- 7.53 ppm (5H, *m*) arising from the aromatic CH groups and at δ_H 9.84 ppm (1H, *s*) for the NH group. The ^{13}C-NMR spectrum of **3a** showed 7 distinct resonances arising from the CCl_3 group (δc 91.18 ppm), aromatic carbons (δc 126.31, 129.42, 130.37 and 135.37 ppm), 2C=O (δc 159.83 and 170.53 ppm). The characterization data of the products are given below.

3. Experimental section

All starting materials and solvents were purchased from Merck (Germany) and Fluka (Switzerland) and were used without further purification. Melting points were determined using an electrothermal 9100 apparatus and were uncorrected. IR spectra were recorded on a Jasco FT-IR 6300 spectrometer. The ^{1}H-NMR and ^{13}C-NMR spectra were measured ($CDCl_3$ solution) with a Bruker DRX-250 Avance spectrometer at 250.13 and 62.90 MHz, respectively. The elemental analyses were realized using a Heraeus CHN-O-rapid analyzer.

General procedure for the synthesis of 3a-c

To a magnetically stirred solution of trichloroacetyl isocyanate (**2**, 1 mmol) in CH_2Cl_2 (5mL) was added 2-naphthalenethiol or thiophenol derivatives (**1**, 1mmol) at -10ºC. The mixture was stirred at room temperature for 1-2 hours. Then the mixture was filtrated, and the products **3a-c** were obtained.

***S*-phenyl (trichloroacetyl)carbamothioate (3a):** White solid, yield: 100%; m.p. 152.3- 153-5 ºC; Anal. Calcd. for $C_9H_6Cl_3NO_2S$: C, 36.20; H, 2.03; N, 4.69. Found: C, 36.33; H, 2.00; N, 4.62; IR (KBr, cm^{-1}): 3328 (NH), 1762 (C=O), 1661 (C=O), 1441 (C-N), 866 and 832 (C-Cl, Str.), 680 (C-S), 470 (C-Cl, bending); ^{1}H-NMR (250.13 MHz, $CDCl_3$, δ / ppm): 7.40- 7.53 (5H, *m*, aromatic CH), 9.84 (1H, *s*, NH); ^{13}C- NMR (62.90 MHz, $CDCl_3$, δ / ppm): 91.18 (CCl_3), 126.31, 129.42, 130.37, and 135.37 (aromatic carbons), 159.83 and 170.53 (2C=O).

***S*-(4-chlorophenyl) (trichloroacetyl) carbamothioate (3b):** White solid, yield: 98%; m.p. 130.5- 132.1 ºC; Anal. Calcd. for $C_9H_5Cl_4NO_2S$: C, 32.46; H, 1.51; N, 4.21. Found: C, 32.43; H, 1.53; N, 4.18; IR (KBr, cm^{-1}): 3325 (NH), 1738 (C=O), 1667 (C=O), 1459 (C-N), 857 and 823 (C-Cl, Str.), 680 (C-S), 484 (C-Cl, bending); ^{1}H-NMR (250.13 MHz, $CDCl_3$, δ / ppm): 7.35-7.51 (4H, *m*, aromatic CH), 9.66 (1H, *s*, NH); ^{13}C-NMR (62.90 MHz, $CDCl_3$, δ / ppm): 91.09 (CCl_3), 124.65, 129.70, 136.52 and 136.90 (aromatic carbons), 159.75 and 169.46 (2C=O).

***S*-naphtalen-2-yl (trichloroacetyl) carbamothioate (3c):** White solid, yield: 97%; m.p. 150.4- 151.8 ºC; Anal. Calcd. for $C_{13}H_8Cl_3NO_2S$: C, 44.79; H, 2.31; N, 4.02. Found: C, 44.84; H, 2.36; N, 3.98; IR (KBr, cm^{-1}): 3301 (NH), 1744 (C=O), 1671 (C=O), 1473 (C-N), 860 and 820 (C-Cl, Str.) 674 (C-S), 471 (C-Cl, bending); ^{1}H-NMR (250.13 MHz, $CDCl_3$, δ / ppm): 7.45- 8.10 (7H, *m*, aromatic CH), 9.41 (1H, *s*, NH); ^{13}C- NMR (62.90 MHz, $CDCl_3$, δ / ppm): 91.22 (CCl_3), 123.39, 126.89, 127.74, 127.87, 128.10, 129.17, 131.17, 133.48, 133.70 and 135.49 (aromatic carbons), 150.47 and 169.40 (2C=O).

4. Computational section

In the present study, we have carried out quantum theoretical calculations for the compounds 3a, 3b and 3c using the G3MP2 [28], LC-ωPBE [29], MP2 [30], and B3LYP [31] methods with the 6-311+G(d,p) [32] basis set by the Gaussian 03W program package [33] and calculating its properties. During the beginning stage, we have had an optimized structure (see Figure 1). Then, we have calculated the ^{1}H NMR and ^{13}C NMR chemical shifts using the G3MP2, LC-ωPBE, MP2, and B3LYP methods with the 6-311+G(d,p) basis set for the title compounds (3a, 3b and 3c) [34]. The electronic properties include Energy of the Highest Occupied Molecular Orbital (EHOMO), Energy of the Lowest Unoccupied Molecular Orbital (ELUMO), HOMO-LUMO energy gap (ΔE), ELUMO, natural charges, and molecular properties. The optimized molecular structure, HOMO and LUMO surfaces have been visualized using GaussView 03 program [35, 36]**.**

4-1. IR spectroscopy

Harmonic vibrational frequencies of the title compounds were calculated using the G3MP2, LC-ωPBE, MP2, and B3LYP methods with the 6-311+G(d,p) basis set. The vibrational frequencies assignments were made using the GaussView program. Some of the characteristic frequencies are given in Table 2- 4. The harmonic frequencies calculated by B3LYP are usually higher than the corresponding experimental values due to the approximate treatment of the electron correlation, anharmonicity effects and basis set deficiencies [37].

For the title compound **(3a)**, the strong band at 3328 cm^{-1} in the FT-IR spectrum is assigned as *ν* N-H mode. The calculated values for this mode are 3321.11, 3315.50, 3322.25 and 3205.56 cm^{-1} for G3MP2, LC-ωPBE/6-311+G(d,p), B3LYP/6-311+G(d,p) and MP2/6-311+G(d,p), respectively.

For the title compound **(3a)**, the strong band at 1762 cm^{-1} in the FT-IR spectrum is assigned as *ν*C=O mode. The calculated values for this mode are the same results for G3MP2, LC-ωPBE/6-311+G(d,p), B3LYP/6-311+G(d,p) and MP2/6-311+G(d,p), respectively. The B3LYP/6-311+G(d,p) computation predicts this vibrational mode in *ν*C-S at 679.25 cm^{-1} for 3a, 679.02 cm^{-1} for the compound 3b and 673.99 cm^{-1} for the compound 3c. This observed frequency coincides well with the expected value [38]. There has been an excellent agreement between experimental and theoretical results for all used methods. In order to compare this agreement, the correlation graphic based on the theoretical and experimental data has been investigated. A small difference between the experimental and calculated vibrational modes is observed. This difference may be due to intermolecular hydrogen bonding formation. Also, the experimental results belong to a solid phase, and theoretical calculations belong to the isolated gaseous phase.

TABLE 2. The selected experimental and theoretical frequencies of the title compounds using G3MP2, LC-ωPBE/6-311+G(d,p), B3LYP/6-311+G(d,p) and MP2/6-311+G(d,p) for compound 3a, 3b and 3c.

Experimental wavenumbers by FT-IR (cm^{-1})			**Calculated vibrational wavenumbers by HF and DFT (cm^{-1})**			
			G3MP2	LC-ωPBE/6-	B3LYP/6-	MP2/6-311+G(d,p)

				311+G(d, p)	311+G(d, p)	
Assigments 3a	N-H	3328	3321.11	3315.50	3322.25	3205.56
	C=O	1762	1725.17	1757.21	1761.23	1747.21
	C=O	1661	1614.22	1631.32	1660.01	1621.77
	C-N	1441	1414.25	1452.11	1445.23	1470.68
	C-Cl Str	866 832	862.14 827.62	861.47 822.58	863.25 831.99	851.98 832.55
	C-S	680	671.13	656.58	679.25	696.68
	C-Cl bending	470	472.78	473.12	470.91	475.09
Assigments 3b	N-H	3325	3312.02	3319.85	3323.02	3321.45
	C=O	1738	1721.02	1716.78	1731.65	1341.78
	C=O	1667	1660.87	1669.77	1663.14	1661.21
	C-N	1459	1442.14	1500.14	1441.14	1444.14
	C-Cl Str	857 823	846.37 821.66	850.14 819.99	851.14 820.11	841.14 821.10
	C-S	680	670.04	677.12	679.02	670.02
	C-Cl bending	484	484.46	484.70	484.14	481.21
Assigments 3c	N-H	3301	3321.14	3323.36	3303.21	3330.25
	C=O	1744	1733.01	1740.14	1741.22	1751.25
	C=O	1671	1670.77	1671.36	1672.11	1671.44
	C-N	1473	1471.36	1470.00	1470.65	1470.25
	C-Cl Str	860 820	869.78 821.77	851.36 820.01	857.36 821.98	860.14 821.25
	C-S	674	633.47	632.58	673.99	674.65
	C-Cl bending	471	423.54	470.36	470.74	472.10

4-2. NMR parameters

The calculation of ^{1}H NMR and ^{13}C NMR chemical shifts of compounds 3a, 3b and 3c are computed at G3MP2, LC-wPBE/6-311+G(d,p), B3LYP/6-311+G(d,p) and MP2/6-311+G(d,p) . The experimental and calculated of ^{1}H NMR and ^{13}C NMR chemical shifts of *S*- aryl(trichloroacetyl)carbamothioate derivatives (3a, 3b and 3c) have been demonstrated in Tables 3-5. Based on our calculations and experimental spectra, we have made a reliable one-to-one correspondence between our fundamentals and any of the chemical shifts have been calculated by the G3MP2, LC-ωPBE, MP2, and B3LYP methods with the 6-311+G(d,p) basis set. For the title compound **(3a)** according to in Tables 3-5, the aromatic CH protons appear at 7.40-7.23 ppm, the calculated amounts at LC-wPBE/6-311+G(d,p) and B3LYP/6-311+G(d,p) basis set levels are at 7.40-7.54 and 7.41-7.55 ppm, respectively. Protons of NH appear at $\delta_{N\text{-}H}$ 9.84 ppm, the calculated amounts at LC-wPBE/6-311+G(d,p) and B3LYP/6-311+G(d,p) basis set levels are at 9.80 and 9.83 ppm, respectively. Also, chemical shifts aromatic carbones appear at 126.31, 129.42, 130.37 and 135.37 ppm, the calculated amounts at LC-wPBE/6-311+G(d,p) and B3LYP/6-311+G(d,p) levels are at 127.02, 128.96, 130.11 and 134.96 ppm, and 126.32, 128.99, 130.33 and 134.97 ppm, respectively. The same is true about other compounds in table 4 and 5. For example compound **(3b)** according to in tables 4, the 4H, m, aromatic CH protons appear at δ_{H} 7.35-7.51 ppm, the calculated amounts at LC-wPBE/6-311+G(d,p) and B3LYP/6-311+G(d,p) basis set levels are at 7.26-7.41 and 7.31-7.59 ppm, respectively. Proton of NH appear at $\delta_{N\text{-}H}$ 9.66 ppm, the calculated amounts at LC-wPBE/6-311+G(d,p) and B3LYP/6-311+G(d,p) basis set levels are at 9.43 ppm, and 9.63 ppm respectively. Also, chemical shifts of three carbonyl groups appear at 126.65, 129.70, 136.52 and 136.90 ppm, the calculated amounts at LC-wPBE/6-311+G(d,p) and B3LYP/6-311+G(d,p) levels are at 121.01, 126.47, 132.93 and 135.41 ppm and 126.21, 129.98, 135.99 and 136.12 ppm, respectively.

The compound **(3c)** according to in tables 5, the aromatic CH protons appear at δ_{CH} 7.45-8.10 ppm, the calculated amounts at LC-wPBE/6-311+G(d,p) and B3LYP/6-311+G(d,p) basis set levels are at 7.31-8.01 and 7.41-8.11 ppm, respectively. Proton of NH group appear at δ_{NH} 9.41 ppm, the calculated amounts at LC-wPBE/6-311+G(d,p) and B3LYP/6-311+G(d,p) basis set levels are at 9.39 ppm, and 9.40 ppm respectively. Also, chemical shifts of three carbonyl groups appear at δ_{c} 150.47 and 169.40 ppm, the calculated amounts at LC-wPBE/6-311+G(d,p) and B3LYP/6-311+G(d,p) levels are at 153.41 and 169.22 ppm and 156.89 and 170.36 ppm, respectively.

TABLE 3. Experimentally measured and calculated ^{1}H chemical shifts δ and ^{13}C chemical shifts δ (ppm, vs TMS) using G3MP2, LC-ωPBE/6-311+G(d,p) , B3LYP/6-311+G(d,p) and MP2/6-311+G(d,p) for compound 3a.

^{1}H NMR	**EXP**	**Calculated**			
		G3MP2	**LC-ωPBE/6-311+G(d,p)**	**B3LYP/6-311+G(d,p)**	**MP2/6-311+G(d,p)**
5H, m, aromatic CH	7.40-7.53	7.44-7.59	7.40-7.54	7.41- 7.55	7.44-7.61
1H, s, NH	9.84	9.79	9.80	9.83	9.87
^{13}C NMR	**EXP**	**Calculated**			
		G3MP2	**LC-ωPBE/6-311+G(d,p)**	**B3LYP/6-311+G(d,p)**	**MP2/6-311+G(d,p)**
aromatic carbones	126.31 129.42 130.37 135.37	125.96 128.63 129.99 135.91	127.02 128.96 130.11 134.96	126.32 128.99 130.33 134.97	127.11 129.33 130.31 135.71
C=O(1)	159.83	160.73	160.21	159.84	160.01
C=O(2)	170.53	172.18	171.38	171.08	172.72

TABLE 4. Experimentally measured and calculated ^{1}H chemical shifts δ and ^{13}C chemical shifts δ (ppm, vs TMS) using G3MP2, LC-ωPBE/6-311+G(d,p) , B3LYP/6-311+G(d,p) and MP2/6-311+G(d,p) for compound 3b.

^{1}H NMR	EXP	Calculated			
		G3MP2	LC-ωPBE/6-311+G(d,p)	B3LYP/6-311+G(d,p)	MP2/6-311+G(d,p)
4H, m, aromatic CH	7.35-7.51	7.32-7.99	7.26-7.41	7.31-7.59	7.25-7.89
1H, s, NH	9.66	9.51	9.43	9.63	9.71
^{13}C NMR	EXP	Calculated			
		G3MP2	LC-ωPBE/6-311+G(d,p)	B3LYP/6-311+G(d,p)	MP2/6-311+G(d,p)
aromatic carbones	126.65 129.70 136.52 136.90	125.87 127.93 134.47 135.99	121.01 126.47 132.93 135.41	126.21 129.98 135.99 136.12	126.73 129.46 136.55 136.63
C=O(1)	159.75	159.87	148.56	158.93	159.91
C=O(2)	169.46	167.02	131.88	169.44	170.03

TABLE 5. Experimentally measured and calculate ^{1}H chemical shifts δ (ppm, vs TMS) using G3MP2, LC-ωPBE/6-311+G(d,p), B3LYP/6-311+G(d,p) and MP2/6-311+G(d,p) for compound 3c.

^{1}H NMR	EXP	Calculated			
		G3MP2	LC-ωPBE/6-311+G(d,p)	B3LYP/6-311+G(d,p)	MP2/6-311+G(d,p)
7H, m, aromatic CH	7.45-8.10	7.11-9.11	7.31-8.01	7.41-8.11	7.43-9.03
1H, s, NH	9.41	9.56	9.39	9.40	9.46
^{13}C NMR	EXP	Calculated			
		G3MP2	LC-ωPBE/6-311+G(d,p)	B3LYP/6-311+G(d,p)	MP2/6-311+G(d,p)
aromatic carbones	123.39 126.89 127.74 127.87 128.10 129.17 131.17 133.48 133.70 135.79	118.76 125.34 127.70 127.99 128.11 129.18 132.56 133.47 133.63 135.93	122.98 125.86 127.21 127.97 128.14 129.36 132.11 133.58 133.99 135.79	123.56 126.37 127.65 127.93 128.12 129.28 131.98 133.11 133.69 135.83	123.11 126.41 127.33 127.84 128.33 129.01 132.77 133.21 133.97 135.88
C=O(1)	150.47	151.12	153.41	156.89	153.11
C=O(2)	169.40	169.25	169.22	170.36	169.41

The synthesis of organic compounds increasingly uses computational chemistry approaches to model and understand molecular phenomena. Calculations are employed to rationalize reaction outcomes, predict how a new system will perform, and inform synthetic plan. As a result, new insights into the interactions of fundamental chemical forces have emerged that advance the field of complex small and large molecule synthesis. This review presents four examples of computational techniques used in the synthesis of organic compounds, and discusses the unique perspectives afforded by these quantitative analyses. We use mathematical algorithms, statistics, and large databases to integrate chemical theory and In addition, a thorough understanding of the synthesized products can be achieved by a careful examination of the structure and reactivity of the compounds through homo and lumo orbitals investigations and molecular softness and hardness.

There is an excellent agreement between experimental and theoretical results for all used methods. In order to compare this agreement, the correlation graphic based on the theoretical and experimental data has been investigated. The correlation value (R^2) for compounds at G3MP2, LC-wPBE/6-311+G(d,p), B3LYP/6-311+G(d,p) and MP2/6-311+G(d,p) have been represented in Table 6. There is an excellent agreement between experimental and theoretical results [34]. A small difference between the experimental and calculated vibrational modes has been observed. This difference may be due to the intermolecular hydrogen bonding formation. Furthermore, the experimental results belong to a solid phase, and theoretical calculations belong to the isolated gaseous phase.

TABLE 6. Correlation of calculated and experimental ^{1}H NMR, ^{13}C NMR and IR of the compounds.

Compounds		G3MP2	LC-ωPBE/6-311+G(d,p)	B3LYP/6-311+G(d,p)	MP2/6-311+G(d,p)
3a	**IR**	0.9986	0.9999	0.9995	0.9997
3b		0.9996	0.9975	0.9999	0.9998
3c		0.9977	0.9995	0.9992	0.9975
3a	**HNMR**	0.9986	0.9999	0.9988	0.9990
3b		0.9970	0.9997	0.9983	0.9991
3c		0.9975	0.9989	0.9991	0.9974
3a	**CNMR**	0.9983	0.9989	0.9990	0.9998
3b		0.9986	0.9998	0.9998	0.9999
3c		0.9953	0.9995	0.9995	0.9978

Quantum chemical methods are significant in obtaining information about molecular structure and electrochemical behavior. A frontier molecular orbitals (FMO) analysis was carried out for the compounds using the B3LYP/6-311+G(d,p) level. FMO results such as EHOMO, ELUMO and the HOMO-LUMO energy gap (Eg) of the title compounds are summarized in Table 7. The energy of the LUMO, and HOMO and their energy gaps reflect the chemical reactivity of the molecule. In addition, the HOMO can act as an electron donor and the LUMO as an electron acceptor. Higher HOMO energy

(EHOMO) for the molecule indicates a higher electron-donating ability to an appropriate acceptor molecule with a low-energy empty molecular orbital. [35, 36] As shown in Figure 1. the HOMO energy of the compound 3c has the highest value (-0.26496eV). A large energy gap implies the high stability for the molecule. The calculated values of the HOMO–LUMO energy gap (Eg) for the structures 3a, 3b and 3c are 0.29, 0.17 and 0.15 eV, respectively. DOS plots [38] also demonstrate the calculated energy gaps (Eg) for the compounds 3a, 3b and 3c (see Figure 1). It is obvious that the energy gap of the compound 3a is the highest (0.29eV), and therefore it is less reactive than the other structures. Meanwhile, the energy gap of the compound 3c is the lowest (0.15 eV), which indicates that it is the most reactive. As presented in Figure 2 charge transfer can take place within the three molecules.

Detailed information about quantum molecular descriptors of title compounds such as ionization potential, electron affinity, global hardness, electronic chemical potential and electrophilicity are calculated and listed in Table 7.

Table 7. The calculated electronic properties of the compounds 3a, 3b and 3c using B3LYP/6-311+G(d,p) level of theory.

Property	**3a**	**3b**	**3c**
HF (Hartree)	-2330.80	-2790.42	-2484.48
Dipole moment (Debye)	3.33	1.70	3.67
Point Group	C1	C1	C1
E_{HOMO} (eV)	-0.35	-0.26	-0.24
E_{LUMO} (eV)	-0.05	-0.09	-0.08
Eg (eV)	0.29	0.18	0.16
***I* (eV)**	0.35	0.26	0.24
***A* (eV)**	0.05	0.087	0.08
***χ* (eV)**	0.38	0.31	0.28
***η* (eV)**	0.32	0.22	0.20
***μ* (eV)**	-0.20	-0.18	-0.16
***ω* (eV)**	0.06	0.07	0.06
***S* (eV)**	1.55	2.26	2.52

The first ionization potential(I) and electron affinity (A) can be expressed through HOMO and LUMO orbital energies by connecting it with Hartree Fock SCF theory and invoking Koopmans' theorem [39] as I=-EHOMO,A=- ELUMO. Chemical hardness (η=I _ A/2) is an important property that indicates the molecular stability and reactivity [40]. A hard molecule has a large energy gap (Eg) and a soft molecule has a small energy gap (Eg) [41]. The chemical hardness (η) values of the compounds 3a, 3b and 3c are 0.321, 0.221 and 0.198 eV respectively. Compound 3a has the highest chemical hardness (η = 0.321 eV), and therefore, it is a hard, less reactive molecule with a high energy gap (Eg= 0.29 eV). Electronic chemical potential (μ=-(I + A)/2) is a form of potential energy that can be absorbed or released during a chemical reaction and that may also change during a phase transition [42- 44]. Electrophilicity (ω) measures the stabilization in energy when the system acquires an additional electronic charge from the environment. The electrophilicity index (ω=μ2/2η) contains information about both electron transfer (chemical potential) and stability (hardness) and is a better descriptor of global chemical reactivity [45]. The higher the value of the electrophilicity index, the higher the capacity of the molecule to accept electrons. The electrophilicity index for the compounds 3a, 3b and 3c is 0.06309, 0.07018 and 0.06546 eV, respectively. The compound 3b has the highest electrophilicity index; therefore it has a high capacity for accepting electrons. The dipole moment (μD) is a good measure of the asymmetric nature of a molecule. The size of the dipole moment depends on the composition and dimensionality of the 3D structures. As shown in Table 7, all structures have a high value of dipole moment and point group of C1, which indicates that there is no symmetry in the structures. The dipole moment of the compound 3c (B3LYP/6-311+G(d,p)=3.6679 Debye) is higher than those of the compounds 3a and 3b (3.3314 and 1.7041 Debye, respectively). The high value for 3c is due to its asymmetric character.

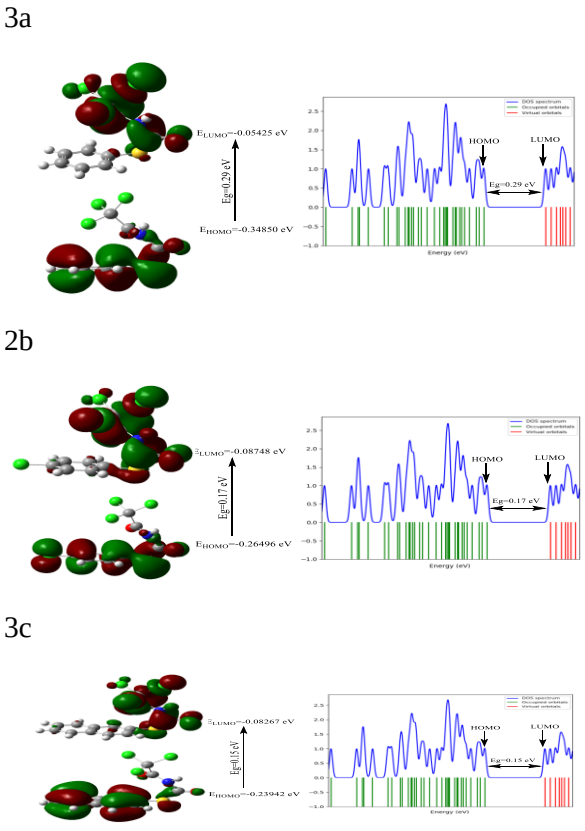

FIGURE 1. Calculated frontier molecular orbitals of compounds 3a, 3b and 3c (Eg: energy gap between LUMO and HOMO) and calculated DOS plots of the title compounds(using the B3LYP/6-311+G(d,p)).

4-3. Thermodynamic analysis

The total energy of a molecule consists of the sum of translational, rotational, vibrational and electronic energies. The statistical thermochemical analysis of title compounds is carried out considering the molecule to be at room temperature of 25°C and 1 atmospheric pressure. The thermodynamic parameters, such as zero point vibrational energy, rotational constant, heat capacity (C) and the entropy (S) of the title compound by B3LYP/6-311+G(d,p) level have been listed in Table 8. According to Table 8, the calculated values for compound 3c is larger than compounds 3a and 3b, therefore compounds 3b and 3a have maximum stability compared to compound 3c due to forming the intramolecular hydrogen bonding.

Table 8. Thermodynamic parameters of the 3a, 3b and 3c molecules using the B3LYP/6-311+G(d,p) level.

	3a	3b	3c
Zero-point correction[a]	0.136679	0.126993	0.183178
Thermal correction to Energy[b]	0.152498	0.144066	0.201638
Thermal correction to Enthalpy[c]	0.153443	0.145011	0.202582
Thermal correction to Gibbs Free Energy[d]	0.089478	0.076901	0.132090
Sum of electronic and zero-point Energies[e]	-2330.66428	-2790.295	-2484.2958
Sum of electronic and thermal Energies[f]	-2330.64846	-2790.278	-2484.2773
Sum of electronic and thermal Enthalpies[g]	-2330.64751	-2790.277	-2484.2764
Sum of electronic and thermal Free Energies[h]	-2330.71148	-2790.346	-2484.3469
E (Thermal)[i]	95.694	90.403	126.529
CV[j]	56.105	59.963	67.893
S[k]	134.624	143.349	148.363

[a-h]Hartree/Particle, [i]KCal/Mol, [j,k] Cal/Mol-Kelvin

4-4. Molecular electrostatic potential (MEP)

The molecular electrostatic potential (MEP) was calculated by the B3LYP/6-311+G(d,p) level. The MEP is related to the electronic density and is a very useful descriptor in understanding sites for electrophilic attack and nucleophilic reactions as well as hydrogen bonding interactions. [45] Negative regions (red color) of the MEP are related to electrophilic reactivity and the positive (blue color) region is related to nucleophilic reactivity, as shown in Figure 2. molecular electrostatic potential (MEP) surface aims at locating the positive and negative charged electrostatic potential in the molecule. In each MEP surface, there is a color scale which indicates the negative and positive value. The red color is a sign of the negative extreme and the blue color depicts the positive extreme. The red color with a negative sign indicates the minimum electrostatic potential (that means it is bound loosely or excess electrons) and it acts as an electrophilic attack. The blue color also indicates the maximum of electrostatic potential, and it acts the opposite.

Starting from the above note, If we plot all MEP surfaces with all iso-surface values, we see only the top surface. It is observed from the MEP map in Figure 2 that the nitrogen-bonded nitrogen atoms in the N-H group and the oxygen atoms in the carbonyl groups (C=O) of the rings are negative regions in all compounds because in the resonance form of the N-H group, the oxygen atoms have a negative charge and the nitrogen atom has a positive charge, and in the resonance form of the carbonyl groups, the oxygen atoms have a negative charge and the carbon atom has a positive charge. So oxygen atoms are sites for electrophilic activity. The nitrogen atoms in the ring, which are attached to carbonyl lethal electron groups, are also positively charged, therefore, nitrogen atoms are sites for nucleophilic attraction. As such these sites give information about the regions where the compounds can have strong intermolecular interactions.

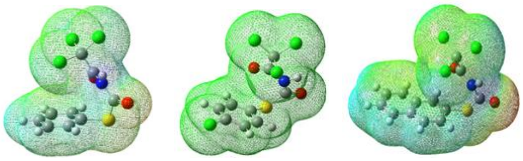

3a 3b 3c

FIGURE 2. Molecular electrostatic potential (MEP) maps of the title compounds calculated using the B3LYP/6-311+G(d,p) level.

5. Conclusion

In the present study, the two-component reaction between 2-naphthalenethiol or thiophenol derivatives, and trichloroacetyl isocyanate to produce *S*-aryl (trichloroacetyl)carbamothioate derivatives was reported. Nevertheless, we believe that the reported method offers a mild, simple, safe, clean and flexible method for the preparation of *S*-alkyl (aryl)carbamothioates derivatives. These compounds of the products were confirmed by IR, ^{1}H NMR, ^{13}C NMR, and elemental analyses. The IR spectra data and ^{1}H NMR and ^{13}C NMR chemical shifts computations of the compounds in the ground state were calculated. There was an excellent agreement between experimental and theoretical results. FMOs, DOS and MEP of the title compounds were investigated by theoretical calculations.

Acknowledgements

The authors are thankful to the Zanjan Branch, Islamic Azad University, for partial support of this work.

References

[1] Q. Meng, H. Luo, Y. Liu, W. Li, W. Zhang and Q. Yao, Synthesis and evaluation of carbamate prodrugs of SQ109 as antituberculosis agents. *Bioorg. Med. Chem. Lett*., 23 (2009) 2808–2810.

[2] J. M. Ferriz and J. Vinsova, Prodrug design of phenolic drugs. *Curr. Pharm. Des*., 16 (2010) 2033–2052.

[3] P. N. Solyev, A. V. Shipitsin, I. L. Karpenko, D. N. Nosik, L. B. Kalnina, S. N. Kochetkov, M. K. Kukhanova and M. V. Jasko, Synthesis and anti-HIV properties of new carbamate prodrugs of AZT. *Chem. Biol. Drug Des*., 80 (2012) 947-952.

[4] Y. H. Yang, A. Voak, S. R. Wilkinson and L.Q. Hu, Design, synthesis, and evaluation of potential prodrugs of DFMO for reductive activation. *Bioorg. Med. Chem. Lett*., 22 (2012) 6583-6586.

[5] C. Gomez, P. Ponien, N. Serradji, A. Lamouri, A. Pantel, E. Capton, V. Jarlier, G. Anquetin and A. Aubry, Synthesis of gatifloxacin derivatives and their biological activities against mycobacterium leprae and mycobacterium tuberculosis. *Bioorg. Med. Chem*., 21 (2013) 948-956.

[6] (a) A. Goel, S. J. Mazur, R. J. Fattah, T. L. Hartman, J. A. Turpin, M. Huang, W. G. Rice, E. Appela and J. K. Inman, Benzamide-based thiolcarbamates: a new class of HIV-1 NCp7 inhibitors. *Bioorg. Med. Chem. Lett*., 12 (2002) 767-770. (b) T. F. Wood and J. H. Gardner, The synthesis of some dialkylaminoalkyl arylthiourethans and thioureas. *J. Am. Chem. Soc.*, 63 (1941) 2741- 2742.

[7] A. W. Erian and S. M. Sherif, The chemistry of thiocyanic esters. *Tetrahedron*, 55 (1999) 7957- 8024.

[8] T. W. Greene and P. G. M. Wuts, Protective Groups in Organic Synthesis, 3rd ed.; Wiley-Interscience: New York, 1999.

[9] N. L. Benoiton, Chemistry of Peptide Synthesis; CRC Press: Boca Raton, 2006.

[10] H. Tilles, Thiolcarbamates. preparation and molar refractions. *J. Am. Chem. Soc*., 81 (1959) 714- 727.

[11] (a) T. Mizuno, I. Nishiguchi and N. Sonoda, Novel synthesis of S-alkyl thiocarbamates from amines, carbon monoxide, elemental sulfur, and alkyl halides in the presence of a selenium catalyst. *Tetrahedron*, 50 (1994) 5669- 5680. (b) T. Mizuno, I. Nishiguchi, T. Okushi and T. Hirashima, Facile synthesis of S-alkyl thiocarbamates through reaction of carbamoyl lithium with elemental sulfur. *Tetrahedron Lett*., 32 (1991) 6867- 6868.

[12] (a) M. S. Newman and H. A. Karnes, The conversion of phenols to thiophenols via dialkylthiocarbamates. *J. Org. Chem.*, 31 (1966) 3980- 3984. (b) R. E. Hackler and T. W. Balko, [3,3]-Sigmatropic rearrangement of allylic dialkylthiocarbamates. *J. Org. Chem.*, 38 (1973) 2106- 2109

[13] W. D. Jones, K. A. Reynolds, C. K. Sperry, R. J. Lachicotte, S. A. Godelski and R. R. Valente, Synthesis of *S*-alkyl and *S*-aryl thiocarbamates, one-pot two-step general synthesis. *Organometallics*, 19 (2000) 1661-1669.

[14] J. Jacob, K. A. Reynolds, W. D. Jones, S. A. Goldeski and R. R. Valente, Nickel-mediated selective carbonylation routes to thiocarbamates. *Organometallics*, 20 (2001) 1028-1031.

[15] H. Kuniyashu, H. Hiraike, M. Morita, A. Tanaka, K. Sugoh and H. Kurosawa, Palladium-catalyzed azathiolation of carbon monoxide. *J. Org. Chem*., 64 (1999) 7305- 7308.

[16] (a) A. Ramazani, Y. Ahmadi, M. Rouhani, N. Shajari and A. Souldozi, The reaction of (*N*-isocyanimino) triphenylphosphorane with an electron-poor *α*-haloketone in the presence of aromatic carboxylic acids: A novel three-component reaction for the synthesis of disubstituted 1,3,4-oxadiazole derivatives. *Heteroat. Chem*., 21 (2010) 368-372. (b) N. Shajari and A. Ramazani, Synthesis of heterocyclic pentavalent phosphorus compounds from phosphitr derivatives and indane-1,2,3-trione. *Phosphorus, Sulfur Silicon Relat. Elem.*, 185 (2010) 1850- 1857.

[17] (a) A. Ramazani, N. Shajari, A. Mahyari and Y. Ahmadi, A novel four-component reaction for the synthesis of disubstituted 1,3,4-oxadiazole derivatives. *Mol. Divers*.,15 (2011) 521- 527. (b) N. Shajari, A. R. Kazemizadeh and A. Ramazani, Synthesis of 5-aryl-*N* -(trichloroacetyl)-1,3,4-oxadiazole-2-carboxamide via three-component reaction of trichloroacetyl isocyanate, (*N* -isocyanimino)triphenylphosphorane, and benzoic acid derivatives. *Turk. J. Chem*., 39 (2015) 874- 879.

[18] (a) S. Dixit, M. Patil and N. Agarwal, Ferrocene catalysed heteroarylation of BODIPy and reaction mechanism studies by EPR and DFT methods. *RSC Adv*., 6 (2016) 47491-47497. (b) L. Zheng, Y. Qiao, M. Lu and J. Chang, Theoretical investigations of the reaction between 1,4-dithiane-2,5-diol and azomethine imines: mechanisms and diastereoselectivity. *J. Org. Biomol. Chem*., 13 (2015) 7558-7569.

[19] (a) A. Bekhradnia and P. O. Norrby, New insights into the mechanism of iron-catalyzed cross-coupling reactions. *Dalton Trans*., 44 (2015) 3959-3962. (b) D. Duca, G. L. Manna and M. R. Russo, Computational studies on surface reaction mechanisms: Ethylene hydrogenation on platinum catalysts. *Phys Chem Chem Phys*., 1 (1999) 1375-1382.

[20] (a) S. G. Smith and J. M. Goodman, Assigning stereochemistry to single diastereoisomers by GIAO NMR calculation: The DP4 probability. *J. Am. Chem. Soc*.,132 (2010) 12946- 12959. (b) Z. Yang, P. Yu and K. N. Houk, Molecular dynamics of dimethyldioxirane C–H oxidation. *J. Am. Chem. Soc*., 138 (2016) 4237- 4242.

[21] (a) P. E. Hansen and J. Spanget-Larsen, Structural studies on Mannich bases of 2-hydroxy-3,4,5,6-tetrachlorobenzene. An UV, IR, NMR and DFT study. A mini-review, *J. Mol. Struct*., 1119 (2016) 235- 239. (b) S. Demir, A. O. Sarioğlu, S. Güler, N. Dege and M. Sönmez, Synthesis, crystal structure analysis, spectral IR, NMR UV–Vis investigations, NBO and NLO of 2-benzoyl-*N*-(4-chlorophenyl)-3-oxo-3-phenylpropanamide with use of X-ray diffractions studies along with DFT calculations. *J. Mol. Struct*., 1118 (2016) 316- 324.

[22] (a) P. Norouzi and R. Ghiasi, Theoretical understanding the effects of external electric field on the hydrolysis of anticancer drug titanocene dichloride. *J. Appl. Spectrosc*., (2020).(b) E. Sheikh Ansari, R. Ghiasi and A. Forghaniha, Computational investigation into the solvent effect on the Diels-Alder reaction of isobenzofuran and ethylene. *Chem. Methodol.*, 4 (2020) 220-233.

[23] (a) R. Ghiasi and A. Peikari, Computational investigation of solvent effect on the structure, spectroscopic properties (13C, 1H NMR and IR, UV), NLO properties and HOMO–LUMO analysis of Ru(NHC)2Cl2(=CH-p-C6H5) complex. *Phys. Chem. Liq*., 55 (2017), 421-431. (b) N. Shajari, R. Ghiasi, N. Aghaei, M. Soltani and A. R. Kazemizadeh, Synthesis and theoretical studies of [2-amino-3-(ethoxycarbonyl)-1, 4-dihydro-1-phenyl-4-pyridinyl] ferrocene derivatives. *Int. J. New Chem*., (2020).

[24] (a) R, Ghiasi and A. Peikari, Solvent effect on the stability and properties of platinum-substituted borirene and boryl isomers: The polarizable continuum model. *Russ. J. Phys. Chem.* B., 90 (2016) 2211-2216. (b) G. R. Ghane Shalmani, R. Ghiasi and A. Marjani, Substituent effects on the structure

and properties of (para-C5H4X)Ir(PH3)3 complexes in the ground state (S0) and first singlet excited state (S1): DFT and TD-DFT investigations. *J. Chem. Res*., (2020).

[25] (a) S. Hossien Saraf and R. Ghiasi, Effect of the solvent polarity on the optical properties in the (OC)5Cr=(OEt)(Ph) complex: A quantum chemical study. *Russ. J. Phys. Chem. A*., 94 (2020) 1047- 1052. (b) R. Ghiasi, H. Pasdar and F Irajizadeh, Understanding the structure, substituent effect, natural bond analysis and aromaticity of osmabenzyne: A DFT stuzdy. *J. Chil. Chem. Soc*., 60 (2015) 2740-2746.

[26] (a) A. Rezaei, R. Ghiasi and A. Marjani, Strong chemisorption of E2H2 and E2H4 (E = C, Si) on B12N12 nano-cage. *J. Nanostructure Chem*., 10 (2020) 179-191. (b) N. Shajari and R. Ghiasi, Theoretical study of tautomerization in 1,5-dimethyl-6-thioxo-1,3,5-triazinane-2,4-dione. *J. Struct. Chem*., 59 (2018) 541-549.

[27] J. L. Kellie and S. D. Wetmore, Selecting DFT methods for use in ONIOM optimizations of enzyme active sites. *Can. J. Chem*., 91 (2013) 559- 572.

[28] L. A. Curtiss, P. C. Redfern, K. Raghavachari, V. Rassolov and J. A. Pople, Gaussian-3 theory using reduced Mo/ller-Plesset order. *J. Chem. Phys*., 110 (1999) 4703-4709.

[29] C. Møller and M. S. Plesset, Note on an approximation treatment for many-electron systems. *Phys. Rev*., 46 (1934) 618- 622.

[30] D. Cremer, In Encyclopedia of Computational Chemistry; Schleyer, P. v. R., Ed.; Wiley: New York, 1998.

[31] R. Krishnan, J. S. Binkley, R. Seeger and J. A. Pople, Self-consistent molecular orbital methods. XX. A basis set for correlated wave functions. *J. Chem. Phys*., 72 (1980) 650-654.

[32] (a) J.-P. Blaudeau, M. P. McGrath, L. A. Curtiss and L. Radom, Extension of Gaussian-2 (G2) theory to molecules containing third-row atoms K and Ca. *J. Chem. Phys*., 107 (1997) 5016- 5021. (b) L. A. Curtiss, M. P. McGrath, J.-P. Blaudeau, N. E. Davis, R. C. Jr. Binning and L. Radom, Extension of Gaussian-2 theory to molecules containing third-row atoms Ga–Kr. *J. Chem. Phys*., 103 (1995) 6104-6113.

[33] M. J. Frisch, G, W. Trucks and H. B. Schlegel, Gaussian 03, Revision B03, Gaussian Inc, PA: Pittsburgh 2003.

[34] L. Shiri, D. Sheikh, A. R. Faraji, M. Sheikhi and S. Seyed Katouli, Selective oxidation of oximes to their corresponding carbonyl compounds by sym-collidinium chlorochromate (S-COCC) as a efficient and novel oxidizing agent and theoretical study of NMR shielding tensors and thermochemical parameters. *Org. Chem*., 11 (2014) 18- 28.

[35] A. Frisch, A. B. Nielson and A. J. Holder, GAUSSVIEW User Manual, Gaussian Inc, PA: Pittsburgh, 2000.

[36] S. Majedi, F. Behmagham and M. Vakili, Theoretical view on interaction between boron nitride nanostructures and some drugs. *J. Chem. Lett.* 1 (2020) 19-24.

[37] F. Piryaei, N. Shajari and H. Yahyaei, Efficient $ZrO(NO_3)_2.2H_2O$ catalyzed synthesis of 1*H*-indazolo [1,2-*b*] phthalazine-1,6,11(13*H*)-triones and electronic properties analyses, vibrational frequencies, NMR chemical shift analysis, MEP: A DFT study. *Heteroat. Chem*., 2020.

[38] S. Guidara, H. Feki and Y. Abid, Vibrational spectral studies and non-linear optical properties of l-leucine l-leucinium picrate: A Density Functional Theory approach. Spectrochim. *Acta. A. Mol. Biomol. Spectrosc*., 115 (2013) 437-444.

[39] S. Shahab, L. Filippovich, M. Sheikhi, R. Kumar, E. Dikusar, H. Yahyaei and A. Muravsky, Polarization, excited states, trans-cis properties and anisotropy of thermal and electrical conductivity of the 4-(phenyldiazenyl) aniline in PVA matrix. *J. Mol. Struct*., 1141 (2017) 703-709.

[40] H. Yahyaei, A. R. Kazemizadeh and A. Ramazani, Synthesis and chemical shifts calculation of *α*-Acyloxycarboxamides derived from indane-1,2,3-trione by DFT and HF methods. *Chin. J. Struct. Chem*. 31 (2012) 1346-1356.

[41] K. G. Vipin Das, C. Yohannan Panicker, B. Narayana, P. S. Nayak, B. K. Sarojini and A. A. Al-Saadi, FT-IR, molecular structure, first order hyperpolarizability, NBO analysis, HOMO and LUMO and MEP analysis of 1-(10H-phenothiazin-2-yl)ethanone by HF and density functional methods. *Acta. A. Mol. Biomol. Spectrosc*., 135 (2015) 162-171.

[42] S. Shahab, L. Filippovich, M. Sheikhi, H. Yahyaei, M. Aharodnikova, R. Kumar and M. Khaleghian, Spectroscopic (polarization, excitedstate, FT-IR, UV/Vis and 1H NMR) and thermophysical investigations of new synthesized azo dye and its application in polarizing film. *Am. J. Mater. Synth. process.*, 5 (2017) 17-23.

[43] M. R. Jalali Sarvestani and S. Majedi, A DFT study on the interaction of alprazolam with fullerene (C20). *J. Chem. Lett.* 1 (2020) 32-38.

[44] M. R. Jalali Sarvestani and Z. Doroudi, Fullerene (C20) as a potential sensor for thermal and electrochemical detection of amitriptyline: A DFT study. *J. Chem. Lett*. 1 (2020) 63-68.

[45] S. Shahab, L. Filippovich, M. Sheikhi, R. Kumar, E. Dikusar, H. Yahyaei and A. Muravsky, Polarization, excited states, trans-cis properties and anisotropy of thermal and electrical conductivity of the 4-(phenyldiazenyl)aniline in PVA matrix. *J. Mol. Struct*., 1141 (2017) 703-709.

How to Cite This Article

Nahid Shajari; Hooriye Yahyaei; Ali Ramazani. "Experimental and computational investigations of some new cabamothioate compounds". Chemical Review and Letters, 4, 1, 2021, 21-29. doi: 10.22034/crl.2020.250849.1081.